Original Article

Integrated Hybrid Renewable Energy Microgrid System with Battery and Super Capacitor Storage for Enhanced Power Sharing

Pradeep Mogilicharla[1], B. Sirisha[2]

[1,2]*Department of Electrical Engineering, University College of Engineering (A), Osmania University, Telangana, India.*

[1]*Corresponding Author : pradeep.mrtgpower@gmail.com*

Abstract - Renewable power sharing with the grid is a complex task as renewable sources are very unpredictable and always vary with respect to available natural sources. Multiple renewable sources connected to a common grid need voltage balancing and stability for power sharing. This paper connects a hybrid renewable source system with energy storage modules to a grid for power sharing. The renewable sources considered are PV panels and PEMFC modules connected along with high-capacity BES and SC units. The PV panels are connected to a Quadratic Boost converter with higher gain and power extraction capability than the conventional boost converter. The BES has the capability to store power during the abundance of renewable power. The stored power can later be utilized when needed during scarcity of renewable power from PV panels and PEMFC. The SC unit has the capability to provide momentary support during any sudden variation on the grid or the source side. This momentary support to the BES unit reduces stress on the battery pack, which extends its health. All the renewable modules and storage units are integrated on the DC side of the system with power sharing through a common DC bus. The common DC bus shares the renewable power to the grid through VSI operated by the SRF controller. The analysis of the proposed hybrid renewable system with storage units is carried out using MATLAB Simulink software. The modeling of the proposed system is implemented using blocks from the 'Powersystems' Simulink library category. The system performance is validated with different operating conditions on the grid and at the renewable source side.

Keywords - Photovoltaic (PV), Proton Exchange Membrane Fuel Cell (PEMFC), Quadratic boost, Battery Energy Storage (BES), Super Capacitor (SC), Voltage Source Inverter (VSI), Synchronous Reference Frame (SRF), MATLAB Simulink.

1. Introduction

With many natural calamities occurring throughout the continents, the natural habitat for humans and living beings is depreciating [1]. This is caused due to the heavy environmental air pollution caused by power generation through fossil fuel sources. The conventional ways of power generation include thermal plants (Coal plants) and diesel generators, etc., which combust fossil fuel for energy [2]. The combustion of these fossil fuels leads to the production of heavy carbon gases with carbon monoxide and dioxide. This leads to environmental temperature raise, which causes global warming, resulting in climatic disasters [3].

In order to reduce the effect of global warming on the environment, renewable power generation is needed. All the conventional fossil fuel generation stations need to be replaced with renewable power generation stations to sustain the global temperatures. Many renewable sources use completely natural sources to generate electrical power [4].

From the available renewable sources, PV plants are considered the most reliable and supple renewable source, which can be installed in any location. The PV plants generate power from solar irradiation natural sources, which is abundant in the morning hours. The next feasible available renewable source is wind farm which generates power using blowing winds [5].

The wind farm comprises a wind turbine driving the machine for power generation. The wind farm is considered more complex and needs a very specific location to be installed, making it less reliable. However, wind farms are placed very far from the main grid for high-rating power generation, transmitting power at longer distances. Of all the available renewable sources like biogas plants, tidal energy, and hydro plants, the only controllable renewable source is PEMFC. The PEMFC is the most reliable renewable source as the power generation can be controlled by the injection of inlet gases (Hydrogen and Oxygen) [6].

This paper considers a hybrid renewable source system with a PV plant and PEMFC unit for sharing renewable power with the grid. For support of the hybrid renewable system, storage elements are also included increasing the sustainability and reliability of the system. Each module or unit is integrated with individual power circuits for voltage boosting pertaining to maintaining the same voltage at the common link [7].

As each unit generates power at different voltage levels, these power circuits are needed and controlled by voltage or current regulators. All the outputs of the power circuits are connected to a common DC bus where the VSI is connected for conversion of DC to 3-ph AC [7]. The outline structure of the proposed hybrid renewable system with a PV plant, PEMFC unit and storage units (BES and SC) is presented in Figure 1.
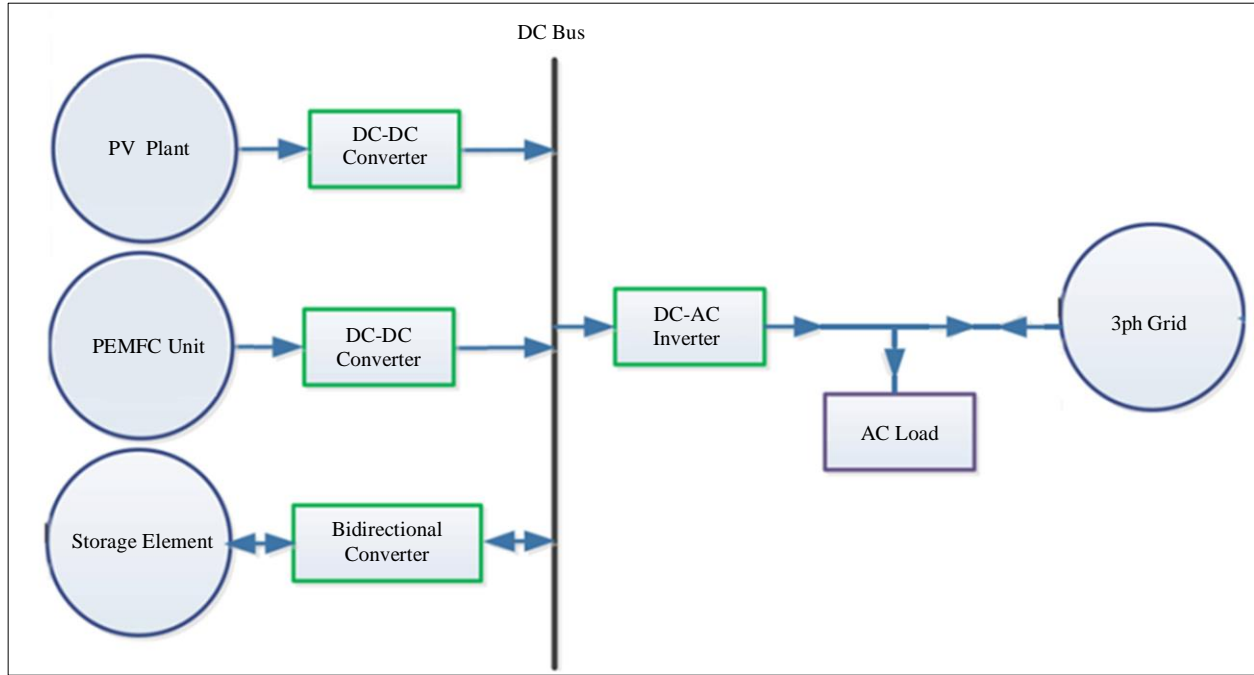

Fig. 1 Structure of proposed hybrid renewable system with storage element

Both the PV plant and PEMFC unit are connected to 'Quadratic boost' and 'conventional boost' DC-DC converters for voltage boosting and stability. The DC-DC converter of the PV plant is controlled by an Incremental conductance-based Maximum Power Point Tracking (MPPT) module. The MPPT extracts maximum power from the PV plant with duty ratio control of the converter switch by taking feedback from the PV plant voltage and current. The DC-DC converter of the PEMFC unit is controlled by current feedback control, which has a PI regulator for generating the duty ratio for the converter switch. The BES and SC storage elements are connected to a bidirectional converter to exchange power between PV or PEMFC.

The BES element is also controlled by the current controller with a PI current regulator, which defines the charging/discharging current of the battery pack. The SC unit converter is integrated with voltage feedback control with a PI voltage regulator for voltage stability at the DC bus. The SRF controller controls the DC-AC inverter at the DC bus by considering signals from 3-ph inverter currents and grid voltages. The grid voltages are considered for synchronization of the inverter to the grid [8]. An AC load is connected at Point

of Common Coupling (PCC), receiving power from either a hybrid renewable system or grid or from both. The main objective is to provide sustainable power to the AC load in any condition of the renewable source, compensating the complete demand and maintaining voltage [9].

Hybrid systems help address the intermittent nature of renewable energy sources. For example, solar energy is only available during the day, while wind energy depends on wind conditions. By combining these two energy sources, a hybrid system can provide a more consistent power supply. Hybrid systems optimize the energy generated from each source. When one source is less productive, the other can compensate, ensuring maximum use of available resources and minimizing waste.

Additionally, because hybrid systems balance energy generation between sources, they reduce the need for extensive and often costly energy storage solutions. For instance, a solar-wind hybrid system can utilize wind energy at night and solar energy during the day, decreasing the reliance on batteries. Moreover, hybrid systems typically require fewer backup sources, such as diesel generators, which

lowers overall greenhouse gas emissions and reduces environmental impact. By integrating multiple renewable sources, these systems lessen our dependence on fossil fuels, contributing to a cleaner energy landscape.

This paper is arranged with an outline structure of the proposed hybrid renewable source system with storage elements connected to the grid in section 1 – introduction. Section 1 defines the elements used in the system for modeling and analysis. Section 2 has the circuit configuration of each unit of the proposed system, and their control modules' design is presented in Section 3. Section 3 contains all the algorithms and control regulators for the proposed system for power exchange between the modules. Section 4 presents the simulation results modelled using MATLAB Simulink software with an analysis of each module's characteristics as per the given operating conditions. The final section 5 presents the conclusion of this paper, which validates the results presented in section 4. The performance endurance of the system for the given operating conditions is finalized in the conclusion, followed by references cited in this paper.

2. System Configuration

The hybrid renewable source with energy storage elements supporting the system for stable power sharing uses multiple power electronics-based circuits. Each source or storage element operates at a different voltage level and cannot be connected directly or in parallel. Therefore, each source is connected with an individual power electronic circuit for power extraction and sharing to the grid or load at desired voltage levels [10]. The power electronic circuits are a combination of passive and active elements that operate to generate the required voltage. The power electronic switches (IGBTs or MOSFETs) are controlled with a dynamic duty ratio for voltage control. Insulated Gate Bipolar Transistor (IGBT) switches are used for application at higher voltage and current rating systems. In contrast, the Metal Oxide Semiconductor Field Effect Transistor (MOSFET) switches are used for high-frequency switching systems.

In the proposed hybrid renewable source with an energy storage elements system, 'Quadratic boost' and 'conventional boost' converters are integrated into the PV plant and PEMFC unit, respectively. The battery pack and supercapacitor are connected to a bidirectional DC-DC converter for power exchange per the renewable power generated. The battery pack is considered a prolonged support unit, and the supercapacitor is taken for momentary support to the system. The BES and SC units are controlled with current regulators, controlling the charge and discharge current magnitude as per the requirement. However, the PV plant has MPPT control for maximum power extraction, irrespective of any operating condition in the system. Even the PEMFC unit is integrated with the current regulator for power delivery control to the system [12]. All the outputs of the power converter circuits are connected to a common DC bus to which a Voltage Source Converter (VSC) is connected for inverting operation. The VSC has six IGBT switches arranged for converting DC voltage from the DC bus to 3-ph AC voltages. The VSC is controlled by an SRF controller for synchronized power sharing to the grid and the local load.
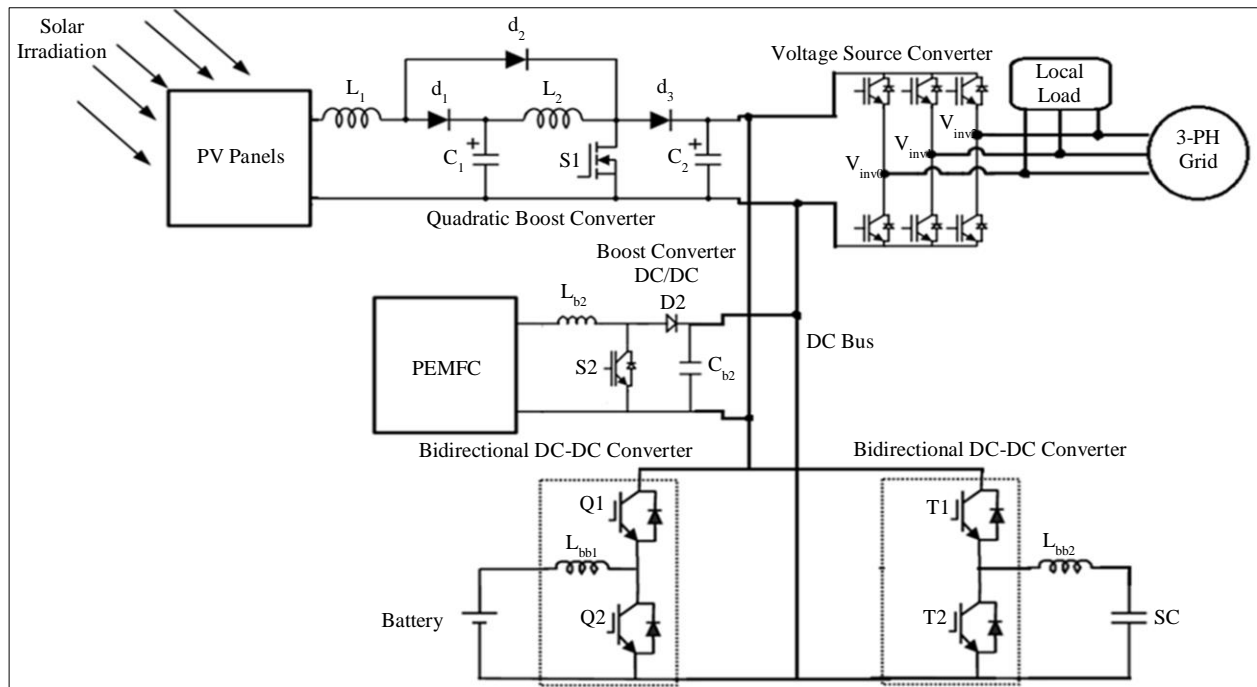

Fig. 2 Circuit topology of the proposed system

The local load is at a common point, consuming power from either renewable sources or the 3-ph grid. The complete circuit structure of the hybrid renewable system with storage units interconnected to the grid is presented in Figure 2.

The 'Quadratic boost' and 'conventional boost' converters of PV panels and PEMFC units are controlled by IGBT switches S1 and S2, respectively [13]. The duty ratio of the switch S1 in the PV plant unit is controlled by the incremental conductance MPPT technique for maximum power extraction. The switch S2 of the PEMFC unit is controlled by current feedback control with regulation on power delivery from the PEMFC source. Each bidirectional converter of the BES and SC unit has two switches, Q1, Q2 and T1 T2, respectively. The Q1, Q2, and T1 T2 switches operated alternatively with a NOT gate connected to one switch. The BES unit operates with current feedback control by taking signal feedback from the battery pack's current measurement. The SC unit is controlled by voltage feedback control with a signal measured from the DC bus supporting the system. The quadratic boost converter is placed with a boosting storage passive element inductor to boost the voltage [14]. The passive elements of the Quadratic boost converter are calculated as:

$$L_1 = \frac{V_{in} + V_{C1}}{di_{L1}} \tag{1}$$

$$L_2 = \frac{-V_{C1}}{di_{L2}} \tag{2}$$

$$C_1 = \frac{i_{L2} - i_{L1}}{dV_{C1}} \tag{3}$$

$$C_2 = \frac{V_o}{R.dV_o} \tag{4}$$

In the given expressions (1) – (4), V_{in} is the PV panels voltage, V_{C1} is the voltage across the capacitor C_1, di_{L1} and di_{L2} are the change in L_1 and L_2 currents respectively, i_{L1} and i_{L2} are the currents through L_1 and L_2, V_o and dV_o are the output voltage and change in the output voltage of the quadratic boost converter, respectively [15]. The 'conventional boost' converter of the PEMFC unit passive element is given as:

$$L_{b2} = R.D \frac{(1-D)^2}{2f_s} \tag{5}$$

Here, R is the equivalent load resistance, D is the average duty ratio of the switch taken as 50%, f_s is the switching frequency of the pulse.

$$L_{bb1\ or\ bb2} = \frac{5(V_{dc} - V_o)V_o}{V_{dc}I_{on}f_s} \tag{6}$$

Here, V_o is the DC link voltage, V_{dc} is the voltage at the storage source and I_{on} is the maximum allowed current through the converter. A capacitive passive element is placed at each output terminal of the converters to reduce the ripple in the output voltage. The output capacitance is given as:

$$C_{b1\ or\ b2} \geq \frac{V_o D}{f_s \Delta V_o R} \tag{7}$$

In the given expression (3) the ΔV_o is the maximum allowable voltage ripple percentage at the output. These passive element values are calculated based on the input voltage, output voltage, maximum current, and average duty ratio, updated in the circuit [16]. Each IGBT and diode switch has a negligible ON resistance in the range 1mΩ with minimal conduction losses.

3. Controller Modules

As mentioned earlier in the previous section, each converter operates with an individual controller that operates according to the system's requirements. The renewable source PV plant is independent and operates irrespective of any requirement of the system. The PV plant generates power using solar irradiation, which varies during the day and is completely zero at night. As the voltage buildup at the output terminals of the PV panels is very low, this voltage needs to be boosted with maximum power extraction [17]. The voltage boosting is, however, achieved by the 'Quadratic boost' converter, and maximum power extraction is achieved by MPPT control [18]. The structure of the Incremental conductance MPPT algorithm is presented in Figure 3.
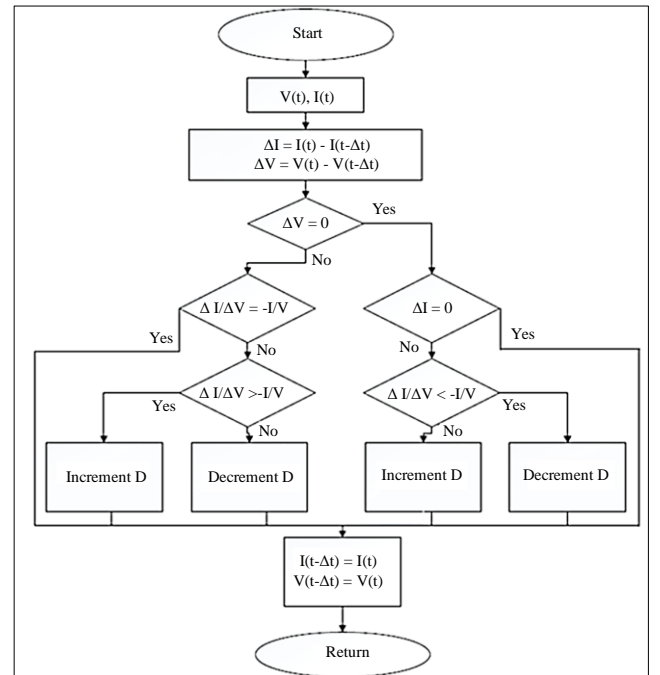

Fig. 3 Incremental conductance MPPT algorithm

As per the algorithm, the duty ratio (D) of the switch S1 is either increased or decreased with respect to changes in the voltage V(t) and current I(t) of the PV plant [19]. The change in voltage and current (ΔV and ΔI) are represented as:

$$\Delta V = V(t) - V(t - \Delta t)$$

$$\Delta I = I(t) - I(t - \Delta t) \qquad (8)$$

Here, $V(t - \Delta t)$ and $I(t - \Delta t)$ are the previous values of the PV plant voltage and current generated by a 'unit delay' module connected at the measured signals. The duty ratio of the switch S1 is varied as per the ΔV and ΔI value generated with respect to time. The increment or decrement of the duty ratio is given as:

$$D = D + \Delta D \begin{cases} If \ \Delta V = 0; \ \Delta I \neq 0; \frac{\Delta I}{\Delta V} < -\frac{I}{V} \\ \Delta V \neq 0; \frac{\Delta I}{\Delta V} > -\frac{I}{V} \end{cases}$$

$$D = D - \Delta D \begin{cases} If \ \Delta V = 0; \ \Delta I \neq 0; \frac{\Delta I}{\Delta V} > -\frac{I}{V} \\ \Delta V \neq 0; \frac{\Delta I}{\Delta V} < -\frac{I}{V} \end{cases}$$

$$D = D \begin{cases} If \ \Delta V = 0; \ \Delta I = 0 \\ \Delta V \neq 0; \frac{\Delta I}{\Delta V} = -\frac{I}{V} \end{cases} \qquad (9)$$

In the final expression, the D remains the same when there is no change in the voltage and current of the PV plant [20]. This D signal is compared to high frequency sawtooth or triangular waveform for pulse generation to the switch S1. For the boost converter of the PEMFC and bidirectional converters of the BES and SC units current and voltage feedback controllers are adopted [21]. The current controller has referenced current signal feedback, and the voltage controller has reference voltage signal feedback [22]. Both the current and voltage controllers of the PEMFC, BES and SC units are presented in Figures 4(a) and (b).
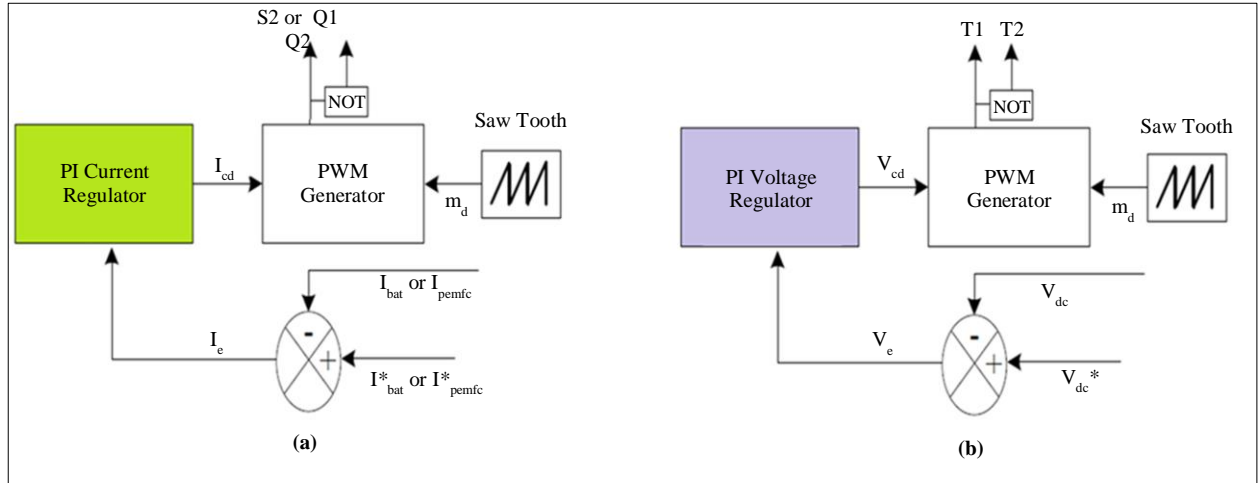

Fig. 4(a) Current controller for PEMFC and BES units, and (b) Voltage regulator for SC unit.

The duty ratios for the PWM generator I_{cd} and V_{cd} are generated by the PI current and voltage regulators, respectively [23]. These signals are calculated as:

$$I_{cd} = \left(I^*_{bat \ or \ pemfc} - I_{bat \ or \ pemfc}\right)\left(K_{pi} + \frac{K_{ii}}{s}\right) \quad (10)$$

$$V_{cd} = (V^*_{dc} - V_{dc})\left(K_{pv} + \frac{K_{iv}}{s}\right) \qquad (11)$$

Here, $I^*_{bat \ or \ pemfc}$ is the reference current value set as per the requirement of the current from the BES or PEMFC unit. V^*_{dc} is the required DC bus voltage value set as per the requirement of the VSC. $I_{bat \ or \ pemfc}$ is the measured current signal of the BES or PEMFC unit and V_{dc} is the measured DC bus voltage. $K_{pi} \ K_{pv}$ are the proportional gains and $K_{ii} \ K_{iv}$ are

the integral gains of current and voltage regulators [23]. These I_{cd} and V_{cd} signals are compared to individual high frequency sawtooth signal (m_d) generating pulses for the converters of PEMFC or BES switches (S1 or Q1 and Q2) and converter of SC unit switches (T1 and T2), respectively.

All the currents from the renewable sources and storage elements are accumulated and injected into the VSC with six IGBT switches connected between the DC bus and the 3-ph grid. The VSC is operated per the DC bus voltage reference set as per the requirement. The SRF controller is a grid-synchronized controller used for power sharing between the storage modules and the 3-ph grid [24]. The structure of the SRF controller with DC bus voltage control and DQ current regulator is presented in Figure 5.
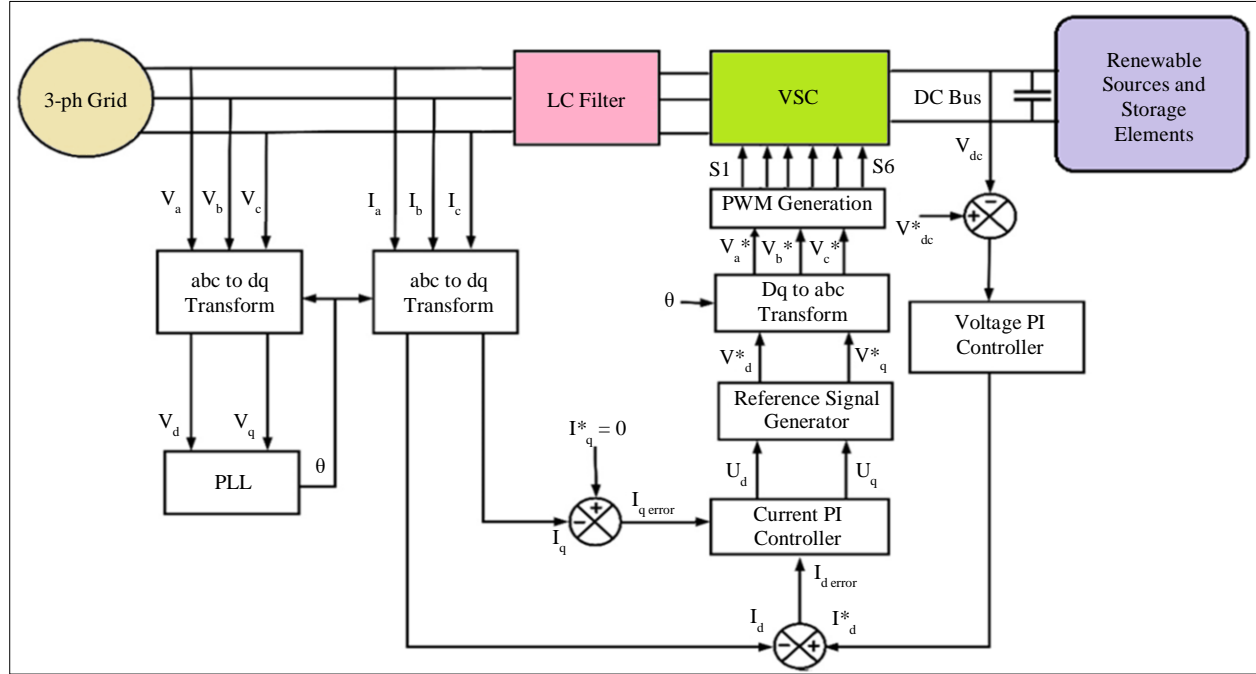
Fig. 5 Structure of the SRF controller for VSC control

The PWM generation needs three reference Sinusoidal signals (V_a* V_b* V_c*) for the generation of PWM pulses for S1 – S6 switches of VSC [24]. These reference signals are generated by Inverse Park's transformation of V_d^* and V_q^* signals. The V_d^* and V_q^* signals are calculated as:

$$V_d^* = U_d + V_d + L\omega I_q \tag{12}$$

$$V_q^* = U_q + V_q - L\omega I_d \tag{13}$$

In the given expressions (8) and (9) V_d V_q and I_d I_q are the dq grid voltage and current components generated from Park's transformation of measured grid voltages and inverter currents. L is the filter inductance value, and ω is the angular frequency (2πf) of the grid. The adjusting components U_d U_q are given as:

$$U_d = (I_d^* - I_d)\left(K_p + \frac{K_i}{s}\right) \tag{14}$$

$$U_q = (I_q^* - I_q)\left(K_p + \frac{K_i}{s}\right) \tag{15}$$

In the given expression (11) I_q^* is taken as '0', representing zero reactive current exchange. K_p K_i are the proportional and integral gains of the current regulator of the SRF controller.

And the I_d^* is calculated as:

$$I_d^* = (V_{dc}^* - V_{dc})\left(K_{pdc} + \frac{K_{idc}}{s}\right) \tag{16}$$

$K_{pdc}K_{idc}$ are the proportional and integral gains of the DC voltage regulator of the SRF controller. As per the V_{dc}^* value, the VSC is controlled, making it possible to maintain the DC link voltage at the given reference value as per the system requirement.

4. Result Analysis

All the units with PV panel and PEMFC connected to 'Quadratic and conventional' boost converters, BES and SC connected to bidirectional converters, VSC connected between DC bus and 3-ph grid and local load are modelled using Simulink library blocks. The blocks for the design are considered from 'Specialized Power Systems' of the 'Electrical' category of the library browser.

The blocks from subsets of 'Passives', 'Sources', 'Control', 'Power Electronics' and 'Sensor and Measurements' are considered for the modeling. The 'PV panels', 'Fuel Cell', 'Battery' and 'Super Capacitor' are considered from the 'Sources' subset. All the parameters of the blocks are updated as per the requirement given in Table 1.

The parameters are updated into the model accordingly, and the simulation are carried out with different operating states of the modules. A comparative analysis is done with the 'Conventional boost' and 'Quadrature Boost' converter in the PV panel.

In the initial case, the solar irradiation is changed from 1000W/m2 to 500W/m2 at 2sec, a total simulation time of 3sec. The graphs of different measurements of the modules

showing the powers, voltages and currents are presented. Figures 6(a) and 6(b) are the characteristics of PV panels and PEMFC units for solar irradiation change conditions, respectively.

Table 1. Configuration parameters

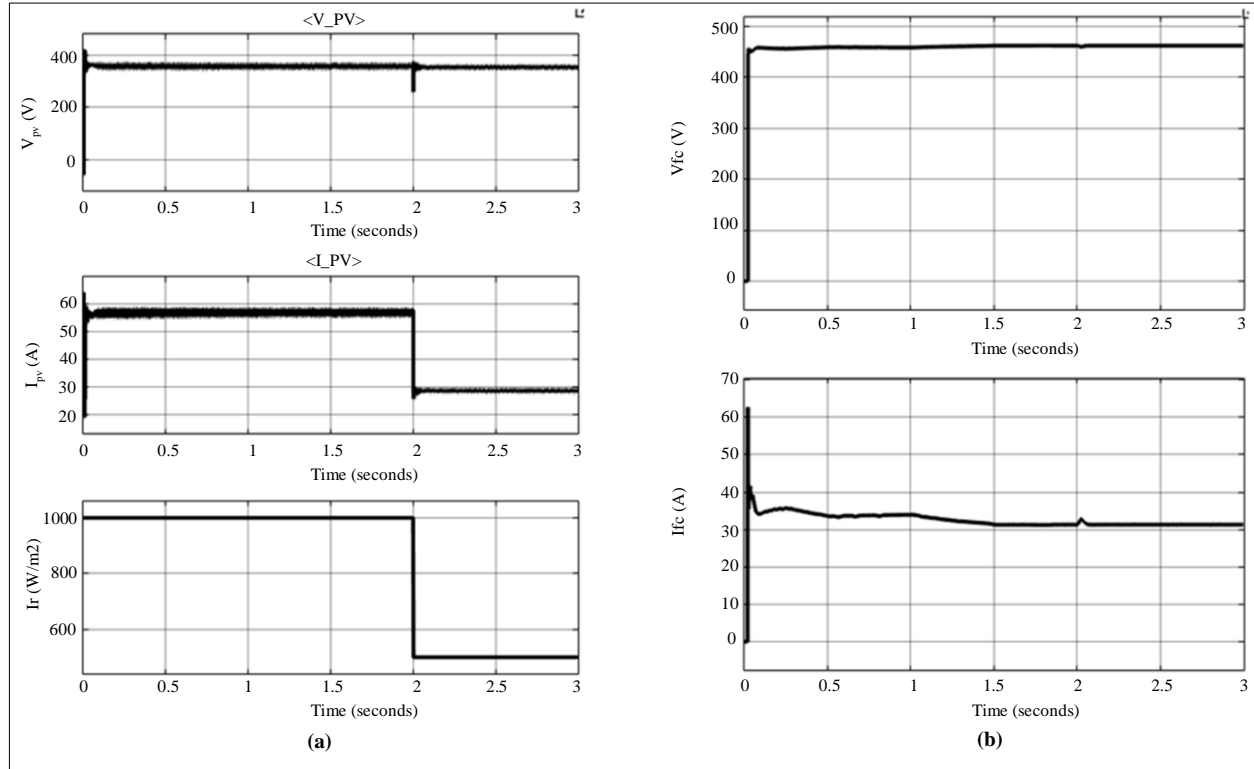| Name of the Unit	Parameters
Grid	132kV, 50Hz, 2500MVA, X/R = 7
PV panels	V_{mp} = 41.5V, I_{mp} = 8.07A, V_{oc} = 49.9V, I_{sc} = 9A, N_s = 9, N_p = 7 Quadratic Boost Converter: $L_1 = L_2$ = 1mH, $C_1 = C_2$ = 100μF
PEMFC	V_{nom} = 400V, I_{nom} = 80A, V_{end} = 166V, I_{end} = 280A Boost Converter: L_{b2} = 1mH, C_{in} = 100μF
BES	V_{nom} = 400V, Capacity = 100Ahr Bidirectional Converter: L_{bb1} = 1mH, R_{igbt} = 1mΩ
SC	V_{rated} = 400V, C_{sc} = 3F, R_{sc} = 8.9mΩ, N_s = 18, N_p = 1
VSC	R_{igbt} = 1mΩ, V_{dcref} = 750V, f_s = 5kHz
Load	Linear Load = 20kW, Non Linear Load = 10Kw

Fig. 6 Characteristics of (a) PV panels, and (b) PEMFC unit for solar irradiation change.

As observed in Figure 6(a), the PV voltage is maintained at 380V for any solar irradiation change, but the current rops from 58A to 29A when the solar irradiation drops at 2sec. With the current control of the P maintained at 30A as per the reference value set in the controller.

The BES and SC unit characteristics with solar irradiation change is presented in Figures 7(a) and 7(b), respectively. The battery voltage is maintained at 403V, and the current

discharge is restricted to 40A by the current controller. The falling slew rate from 80% initial battery SOC depicts the battery discharging. The voltage of the SC is raised from 350V to a rated value of 415V, charging the SC to 100% with a high charging current. The current goes to zero after the SC reaches 100% with no power exchange. Figures 8(a) - 8(f) are the active powers comparison of all the modules connected in the hybrid renewable grid connected system with conventional and quadratic boost converters are presented.
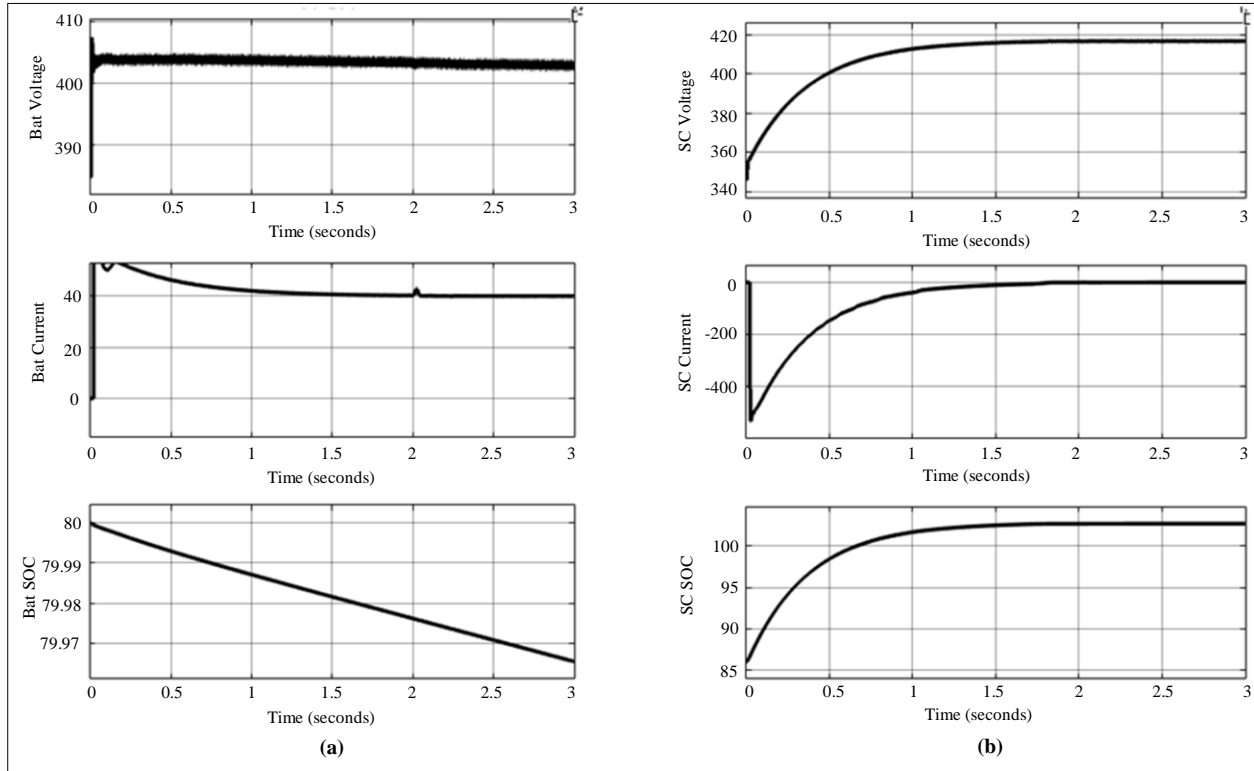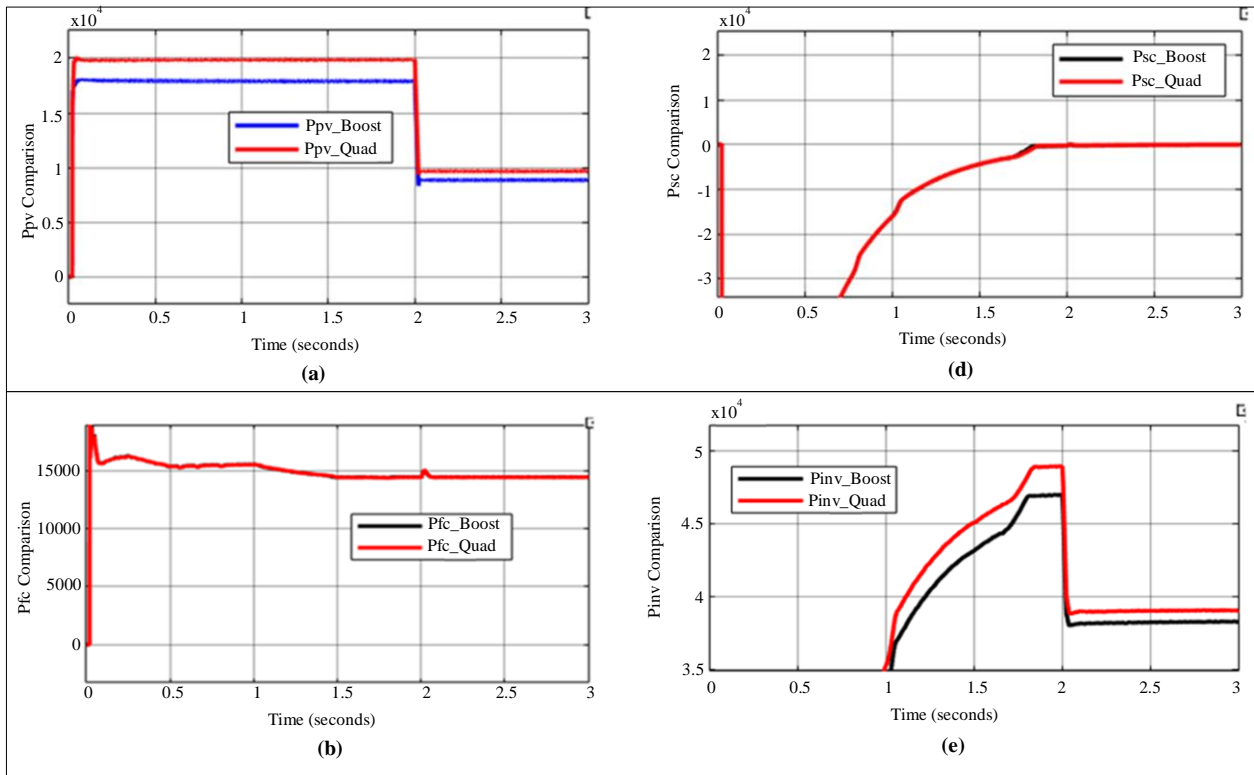
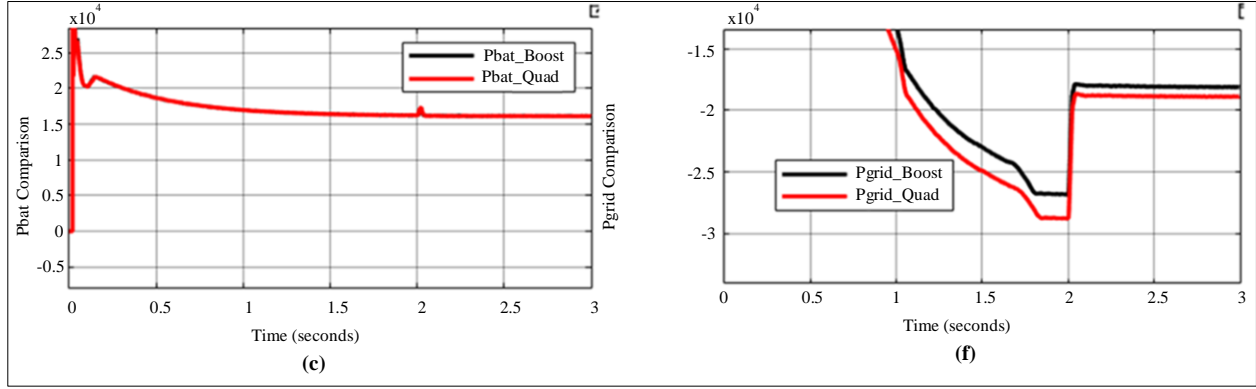**Fig. 7 Characteristics of (a) BES unit, and (b) SC unit for solar irradiation change.**

Fig. 8 Power comparisons of (a) PV panels, (b) PEMFC unit, (c) BES unit, (d) SC unit, (e) Inverter, and (f) Grid for solar irradiation change.
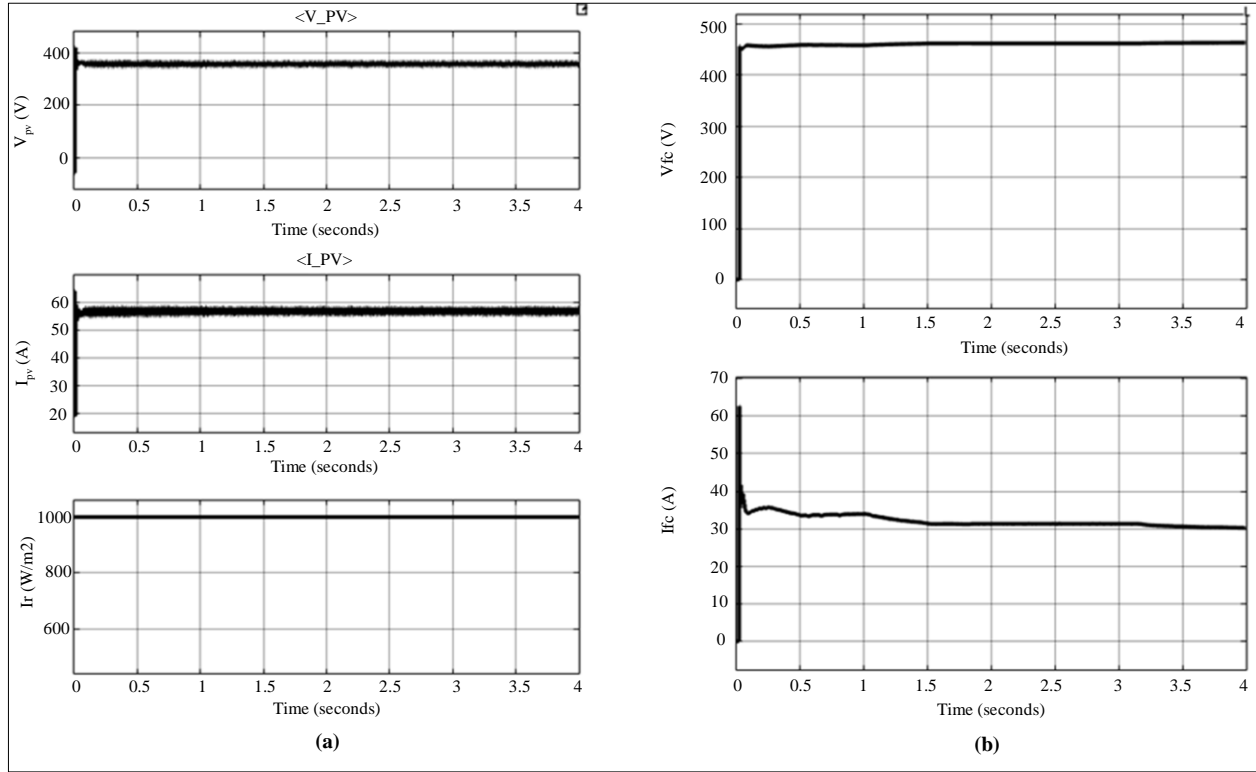

Fig. 9 Characteristics of (a) PV panels, and (b) PEMFC unit for load change.

As per Figure 8(a), the PV panel's power extraction is increased by 2kW when operated with a quadratic boost converter at 1000W/m². The power extraction with a conventional boost converter is 18kW, which is increased to 20kW by the quadratic boost converter.

When the solar irradiation is dropped to 500W/m² the power extraction reduces to half. With a conventional boost converter, the extracted power is 9kW, and the quadratic boost converter is 10kW. The PEMFC and BES powers are maintained at 15kW and 16kW, as observed in Figures 8(b) and 8(c), even during solar irradiation change by the current controller.

After a time of 1.8sec, the SC power sets at zero with no exchange of power from the DC bus, which can be observed in Figure 8(d). As the PV power drops, the inverter's total power injected into the grid is decreased from 48kW to 38kW at 2sec. As per the change in inverter power, the power delivered to the grid has also decreased by 10kW at 2sec. After the local load consumption 20kW from the 48kW inverter power during 0-2sec, the remaining 28kW is injected into the grid. There is an increase of 2kW in grid power delivery due to a quadratic boost converter at the PV panels.

When solar irradiation drops, the grid power delivery is reduced to 18kW, and the PV power drops to 2sec. The negative power direction of the grid power represents grid

injection. The total power delivered by the inverter is increased by 2kW in any condition observed in Figure 8(e). In the next condition, the solar irradiation is maintained at 1000W/m^2 throughout the simulation time of 4sec, and a dynamic load is connected to the grid side. The dynamic load varied at several instants of time. Initially, at 0sec, the load is set with 20kW, which is increased to 25kW at 2.5sec, 30kW at 3sec and 22kW at 3.5sec of the total simulation time of 4sec. The characteristics of the modules and the power comparisons

for the load variation are plotted with respect to time. Figures 9(a) and 9(b) represent the characteristics of the PV panels and PEMFC unit for load change conditions. The current state of both renewable sources is maintained and stable, as there is no change in solar irradiation or the current reference. Even the BES and SC characteristics presented in Figures 10(a) and 10(b) do not change as the reference current and voltage values are maintained the same throughout the simulation.
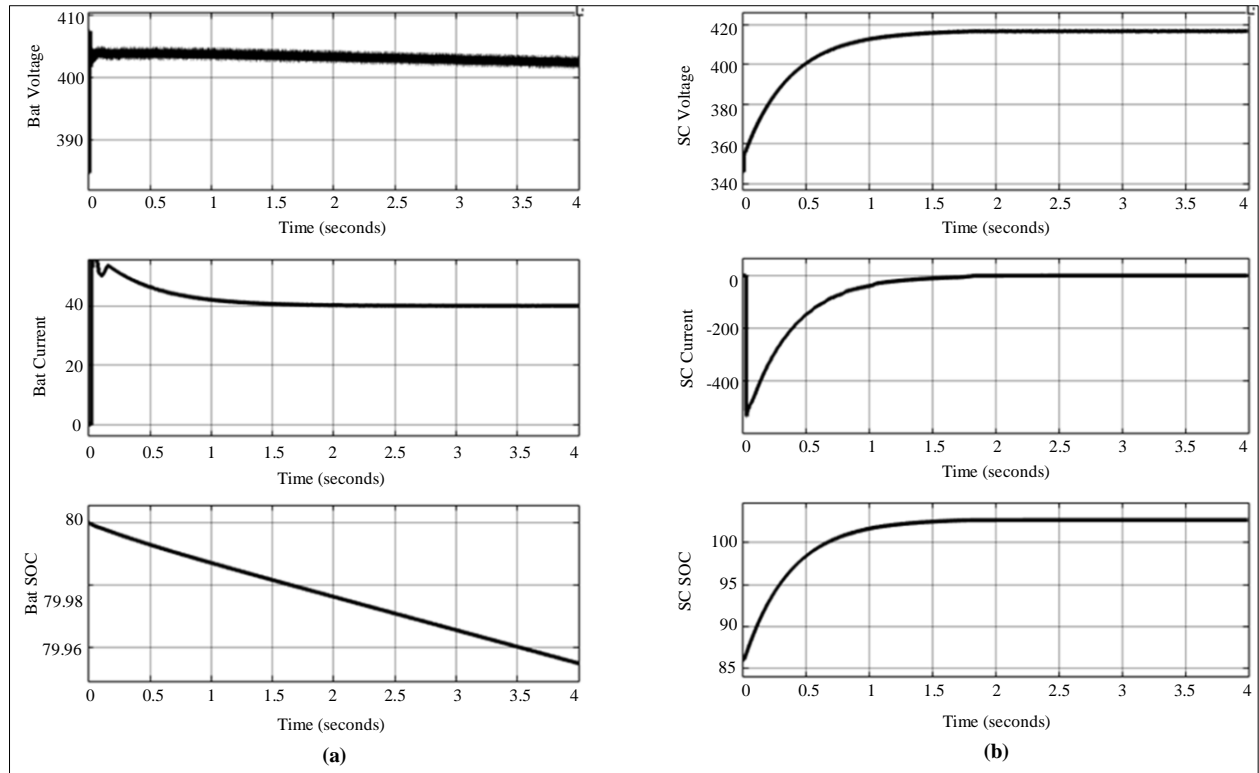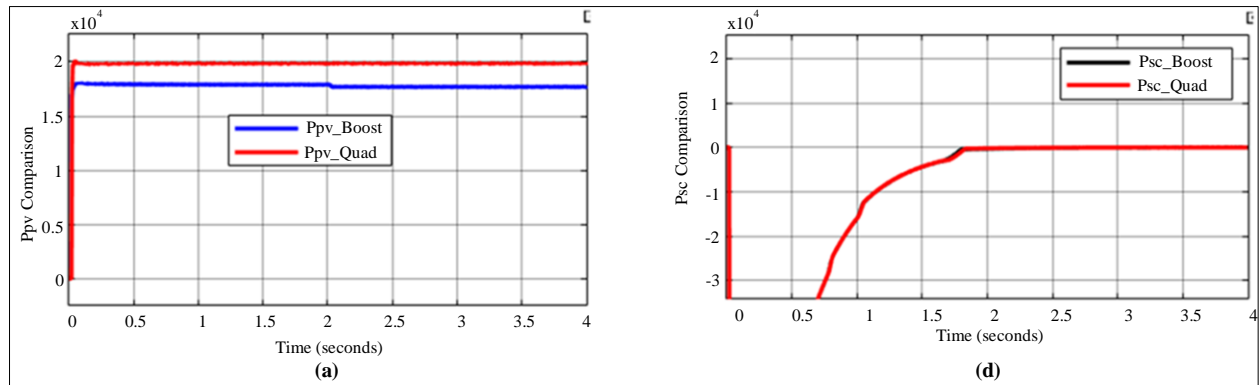

Fig. 10 Characteristics of (a) BES unit, and (b) SC unit for load change.

Figure 11(a)-11(f) represents the active powers of all the system modules with load change conditions. Figure 11(a) shows that the PV panel's power extraction is increased by 2kW, as in the previous case, due to the quadratic boost converter. With no change in the solar irradiation, the power

delivered by the inverter is constant at 48kW, irrespective of load demand. As per the load changes at 2.5, 3 and 3.5secs, the power injected into the grid varies accordingly. The power injected into the grid varies from 28kW to 24kW at 2.5sec, 24kW to 19kW at 3sec and 19kW to 26kW at 3.5sec.
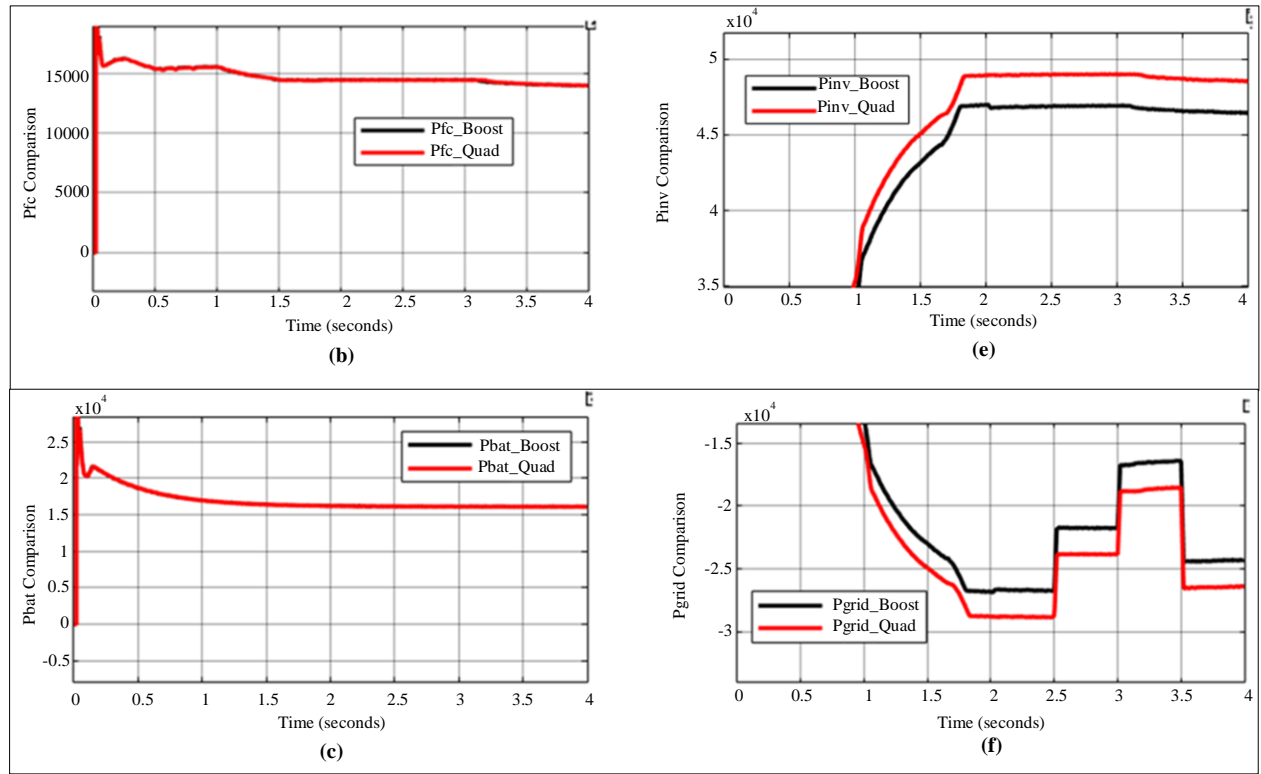
Fig. 11 Power comparisons of (a) PV panels, (b) PEMFC unit, (c) BES unit, (d) SC unit, (e) Inverter, and (f) Grid for load change.

As per the given graphs of the modules, the system is determined to be stable under any given operating conditions. The power from renewable sources is completely extracted and delivered to the grid by multiple power converters in synchronization with the grid. The storage elements provide power to the grid per the references set in the controllers, maintaining stability. As per Figure 11(e), the total power delivered by the inverter is 49kW with a 'quadratic boost converter', which is 2kW higher than the 47kW with a 'conventional boost converter'.

5. Conclusion

The hybrid renewable system with PV panels and a PEMFC unit, along with BES and SC storage elements, is designed in a Simulink environment. The total power from the PV panels is extracted completely by the MPPT algorithm. Excess power of 10% is extracted from the PV panels when the conventional boost converter is replaced with a Quadratic boost converter for the same MPPT algorithm. The PEFC and BES modules share stable power with the DC bus per the given reference current value in the current controllers. The SC unit initially charges with a high current, which stops charging after reaching full SOC. The SC unit provides only momentary support to the system during sudden changes in load or sudden changes in solar irradiation, protecting the BES unit from sudden discharges. It is observed that the excess power from the hybrid renewable system with storage elements is injected into the grid after local load compensation is applied. In any given condition, the synchronization between the inverter and the grid is maintained with no voltage fluctuations in the load or the grid. This system can further be upgraded with a power management algorithm that controls the powers from the storage elements and PEMFC unit as per the PV panel's power and load demand.

References

[1] Kashif Abbass et al., "A Review of the Global Climate Change Impacts, Adaptation, and Sustainable Mitigation Measures," *Environmental Science and Pollution Research*, vol. 29, pp. 42539–42559, 2022. [CrossRef] [Google Scolar] [Publisher Link]

[2] Aadil Gulzar et al., "A Brief Review on Global Warming and Climate Change: Consequences and Mitigation Strategies," *International Journal of Advance Research in Science and Engineering*, vol. 7, no. SI04, 2018. [Google Scolar] [Publisher Link]

[3] Ahmed I. Osman et al., "Cost, Environmental Impact, and Resilience of Renewable Energy under a Changing Climate: A Review," *Environmental Chemistry Letters*, vol. 21, pp. 741-764, 2023. [CrossRef] [Google Scolar] [Publisher Link]

[4] M.A. Russo et al., "Forecasting the Inevitable: A Review on the Impacts of Climate Change on Renewable Energy Resources," *Sustainable Energy Technologies and Assessments*, vol. 52, part C, 2022. [CrossRef] [Google Scolar] [Publisher Link]

[5] Qusay Hassan et al., "A Review of Hybrid Renewable Energy Systems: Solar and Wind-Powered Solutions: Challenges, Opportunities, and Policy Implications," *Results in Engineering*, vol. 20, 2023. [CrossRef] [Google Scolar] [Publisher Link]

[6] Reza Sedaghati, and Mahmoud Reza Shakarami, "A Novel Control Strategy and Power Management of Hybrid PV/FC/SC/Battery Renewable Power System-Based Grid-Connected Microgrid," *Sustainable Cities and Society*, vol. 44, pp. 830-843, 2019. [CrossRef] [Google Scolar] [Publisher Link]

[7] Ishita Biswas, and Prabodh Bajpai, "Control of PV-FC-Battery-SC Hybrid System for Standalone DC Load," *2014 Eighteenth National Power Systems Conference (NPSC)*, Guwahati, India, pp. 1-6, 2014. [CrossRef] [Google Scolar] [Publisher Link]

[8] Seydali Ferahtia et al., "A Hybrid Power System Based on Fuel Cell, Photovoltaic Source and Supercapacitor," *SN Applied Sciences*, vol. 2, 2020. [CrossRef] [Google Scolar] [Publisher Link]

[9] Fahad Alsokhiry, "Grid-Connected Hybrid Renewable Energy System under Various Operating Conditions," *2024 IEEE 8th Energy Conference (ENERGYCON)*, Doha, Qatar, pp. 1-6, 2024. [CrossRef] [Google Scolar] [Publisher Link]

[10] Ibrahem E. Atawi et al., "Recent Advances in Hybrid Energy Storage System Integrated Renewable Power Generation: Configuration, Control, Applications, and Future Directions," *Batteries*, vol. 9, no. 1, 2023. [CrossRef] [Google Scolar] [Publisher Link]

[11] I. Hamdan, Amira Maghraby, and Omar Noureldeen, "Stability Improvement and Control of Grid-Connected Photovoltaic System during Faults Using Supercapacitor," *SN Applied Sciences*, vol. 1, 2019. [CrossRef] [Google Scolar] [Publisher Link]

[12] Hossein Golizedeh et al., "A Quadratic Boost Converter with Continuous Input Current and Suitable for Photo Voltaic Solar Panels," *28th Iranian Conference on Electrical Engineering (ICEE)*, Tabriz, Iran, pp. 1-5, 2020. [CrossRef] [Google Scolar] [Publisher Link]

[13] Jalla Upendar et al., "Implementation and Study of Fuzzy Based KY Boost Converter for Electric Vehicle Charging," *International Journal of Applied Power Engineering (IJAPE)*, vol. 11, no. 1, pp. 98-108, 2022. [CrossRef] [Google Scolar] [Publisher Link]

[14] Antonino Sferlazza, Carolina Albea-Sanchez, and Germain Garcia, "A Hybrid Control Strategy for Quadratic Boost Converters with Inductor Currents Estimation," *Control Engineering Practice*, vol. 103, 2020. [CrossRef] [Google Scolar] [Publisher Link]

[15] M. Al Mamun, Md. Ali Hasan, and Eaqub Khan, "High Voltage Conversion DC-DC Step Up Converter for Fuel Cell Applications," *2017 3rd International Conference on Electrical Information and Communication Technology (EICT)*, Khulna, Bangladesh, pp. 1-4, 2017. [CrossRef] [Google Scolar] [Publisher Link]

[16] Pedro Andrade et al., "Buck-Boost DC-DC Converters for Fuel Cell Applications in DC Microgrids State-of-the-Art," *Electronics*, vol. 11, no. 23, 2022. [CrossRef] [Google Scolar] [Publisher Link]

[17] Ambuj Sharma, Soumya Shubhra Nag, and G. Bhuvaneswari, "Analysis of Conventional Non-Isolated Bidirectional Converters with Smooth Transient Operation," *IEEE Texas Power and Energy Conference (TPEC)*, USA, pp. 1-6, 2021. [CrossRef] [Google Scolar] [Publisher Link]

[18] Liqun Shang, Hangchen Guo, and Weiwei Zhu, "An Improved MPPT Control Strategy Based on Incremental Conductance Algorithm," *Protection and Control of Modern Power Systems*, vol. 5, no. 2, pp. 1-8, 2020. [CrossRef] [Google Scolar] [Publisher Link]

[19] D. Saravana Selvan, "Modeling and Simulation of Incremental Conductance MPPT Algorithm for Photovoltaic Applications," *International Journal of Scientific Engineering and Technology*, vol. 2, no. 7, pp. 681-685, 2013. [Google Scolar] [Publisher Link]

[20] Abdelkhalek Chellakhi et al., "An Enhanced Incremental Conductance MPPT Approach for PV Power Optimization: A Simulation and Experimental Study," *Arabian Journal for Science and Engineering*, vol. 49, pp. 16045-16064, 2024. [CrossRef] [Google Scolar] [Publisher Link]

[21] Ratna Ika Putri, Sapto Wibowo, and Muhamad Rifai, "Maximum Power Point Tracking for Photovoltaic Using Incremental Conductance Method," *Energy Procedia*, vol. 68, pp. 22-30, 2015. [CrossRef] [Google Scolar] [Publisher Link]

[22] Krishnarajsinh A. Jadav, "Design a Residential PV Power System with Battery Energy Storage," *International Journal on Advances in Engineering Technology and Science*, vol. 1, no. 2, pp. 1-6, 2015. [Google Scolar] [Publisher Link]

[23] M.M. Hoque, M.A. Hannan, and A. Mohamed, "Optimal CC-CV Charging of Lithium-Ion Battery for Charge Equalization Controller," *2016 International Conference on Advances in Electrical, Electronic and Systems Engineering (ICAEES)*, Putrajaya, Malaysia, pp. 610-615, 2016. [CrossRef] [Google Scolar] [Publisher Link]

[24] Yuan Mao, Yun Yang, and Kaiyuan Wang, "A Primary-Side Fixed-Frequency CC and CV Output Control for Single-Stage Wireless Battery Chargers with Series Compensation Receivers," *IEEE Transactions on Transportation Electrification*, vol. 10, no. 2, pp. 3407-3415, 2024. [CrossRef] [Google Scolar] [Publisher Link]